Available online at www.sciencedirect.com
ScienceDirect
Journal of Power Sources 158 (2006) 964–976
JOURNAL OF POWER SOURCES
www.elsevier.com/locate/jpowsour

Thermal phenomena during operation of the oxygen cycle in VRLAB and processes that cause them

D. Pavlov *

Institute of Electrochemistry and Energy Systems (CLEPS), Bulgarian Academy of Sciences, Sofia 1113, Bulgaria

Available online 20 December 2005

Abstract

The present paper makes a summary of the results of the investigations on the oxygen cycle (OxCy) performed in this laboratory with the aim to elucidate the processes that take place at the two electrodes of VRLA cells during OxCy operation and the thermal phenomena caused by these processes. It has been established that on constant voltage polarization, the cell reaches a certain state after which its temperature (T) and current (I) begin to increase spontaneously and pass through maxima before reaching stationary values. This phenomenon is called thermal runaway (TRA). These maxima are a result of self-accelerating interrelation established between the rates of the reactions involved in the oxygen cycle at the two electrodes. At high polarization voltages and currents, electrochemical reactions proceed at the positive and negative plates leading to changes in the surface properties and the structures of the PbO_2 and Pb plates as well as in the composition of the electrolyte filling the pores of the active masses. The above changes result in passivation of the PbO_2 electrode, decrease of the rate of O_2 evolution at the positive plates and initiate new chemical exothermic reactions of O_2 reduction at the negative plates. The generated heat causes the cell temperature to rise. If the temperature is higher than 60 °C for a long period of time, this may impair the performance characteristics of the cell. This paper proposes a mechanism of the chemical and electrochemical reactions that proceed at the positive and negative plates during operation of the oxygen cycle (OxCy) and their evolution on constant voltage polarization of the cell. It has been established that there are critical values of T and φ above which the OxCy efficiency declines substantially and thermal phenomena proceed causing TRA.

Keywords: VRLAB; Oxygen cycle; Thermal runaway; Oxygen cycle reactions; Thermal phenomena in VRLAB

1. Introduction

1.1. Electrochemical systems

VRLA batteries consist of two electrochemical systems:

(a) The current generating and accumulating system comprising the $Pb/PbSO_4$ and $PbO_2/PbSO_4$ plates.
(b) Oxygen cycle (OxCy): when the state of charge reaches 70%, H_2O decomposition starts and O_2 is evolved on the positive plates. It passes through the AGM separator and is reduced at the negative plates forming water. The OxCy reduces the water loss during operation of VRLAB.

The reactions involved in the OxCy proceed at the lead and lead dioxide electrodes whose structure, phase composition and physico-chemical properties exert a strong influence on the type and rate of OxCy reactions. The present paper will pay special attention to the interrelation between the above two electrochemical systems.

1.2. Energy transformation during operation of the OxCy

For the OxCy to operate a certain amount of electrical energy has to be introduced into the cell. Part of this energy is returned to the electrical system through the electrochemical reactions that proceed at the two electrodes in the cell. Another part is converted into heat through chemical exothermic reactions. These phenomena are presented schematically in Fig. 1.

Thus, depending on the reversibility of the electrochemical processes, the electrical energy can be partially transformed into heat in the cell. This heat causes the cell temperature to rise and is then dissipated in the surrounding medium through heat exchange. The generated heat is mainly a result of reactions of oxygen reduction at the negative plates and of the Joule effect of the current passing through the cell.

* Tel.: +359 2 9710083; fax: +359 2 8731552.
E-mail address: dpavlov@labatscience.com.

0378-7753/$ – see front matter © 2005 Elsevier B.V. All rights reserved.
doi:10.1016/j.jpowsour.2005.11.004

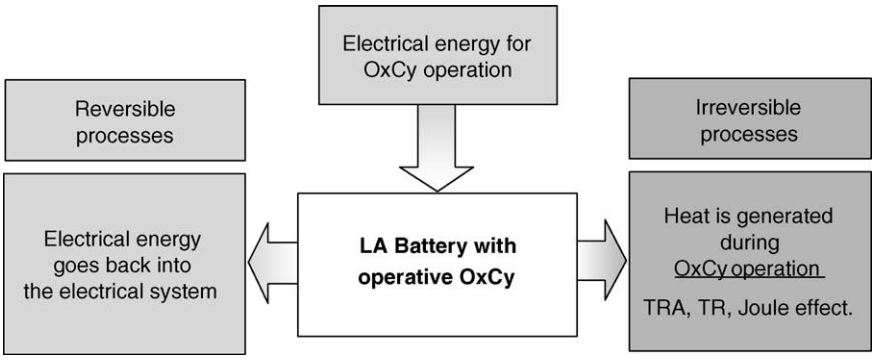

Fig. 1. Schematic representation of the transformations of the electrical energy introduced into the lead–acid cell for the OxCy to operate.

1.3. Types of temperature changes

The lead–acid battery operates normally at temperatures up to 60 °C. During operation of the OxCy the temperature (T) in the cell may rise in two ways (Fig. 2):

(a) Temperature rise: the temperature rises up to a stationary value within a transition period (Tr.p.). When T does not exceed 60 °C (which is the upper temperature limit for normal battery operation), the thermal phenomena would cause no damage to the battery.
(b) Thermal runaway: during the transition period, the temperature passes through a maximum before reaching a stationary value. The temperature maximum on TRA may reach values much higher than 60 °C and thus may cause battery damage. When the temperature maximum reaches 100 °C, colloidal PbO_2 may form, which may penetrate into the separator and cause short circuits between the plates as well as changes in the structure of the Pb and PbO_2 active masses. The polymer battery case and cover swell and the expander is destroyed. In some cases the electrolyte may boil and even a weak explosion may occur in the battery.

1.4. Investigations of the OxCy thermal phenomena

Thermal phenomena have long been in the focus of attention of researchers. Giess and Haering [1,2] have studied the temperature distribution in a VRLA cell using a video imaging system. Pesaran et al. [3–5] have investigated the thermal phenomena using coupled calorimetric–electrochemical device and proposed a battery thermal management system. Culpin [6] has established the influence of separators on TRA. Wagner [7] has studied the influence of thermal phenomena on the performance of VRLAB. Li et al. [8] have conducted research on the influence of T and state of charge on the rate of H_2O recombination during OxCy. Robinson and Tarascon [9] have found that when VRLABs operate at temperatures higher than 60 °C, H_2S and SO_2 are formed within the batteries. Management systems for control of the thermal behaviour of the batteries have also been proposed [10–12].

1.5. Aim of the present paper: to review and summarize the results of the OxCy investigations performed in this laboratory

In a series of earlier papers of our laboratory we determined the energy balance of the OxCy [13] and elucidated the mechanism of the reactions of oxygen evolution at the positive plates [14,15] as well as the mechanism of the reaction of oxygen reduction at the negative plates [16–19]. The present paper will summarize the basic results obtained in the above works [13–19] and will attempt to provide an adequate interpretation of these results and elucidate the mechanism of the reactions that proceed at the two electrodes during operation

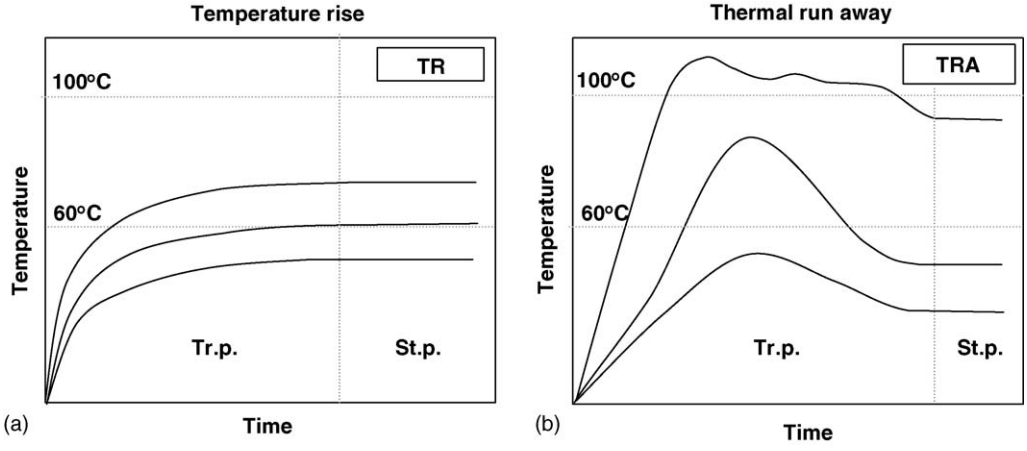

Fig. 2. Changes in cell temperature during the transition period (Tr.p.) until stationary operation (St.p.) of the OxCy.

of the OxCy and their role in the occurrence of the thermal phenomena.

1.6. Experimental

We investigated fully charged cells where only the reactions of the OxCy proceeded. The cells were polarized at constant voltage (six different voltages between 2.40 and 2.65 V increased in 50 mV steps) or by linear sweep voltammetry. The following parameters were measured continuously: cell current (I) and voltage (U), positive and negative plate potentials (φ^+ and φ^-), cell temperature (T) and efficiency of the OxCy. The model cells (2 V/4.5 Ah) and the experimental set up are described in detail in [16]. The testing equipment limited the charging current to 9.5 A ($I = 2C_{10}$ A, where C_{10} is the capacity at 10-h discharge rate.) Each cell was outfitted with a $Ag/AgSO_4$ reference electrode, a thermocouple and a valve. The efficiency of the oxygen cycle was determined from the rate of hydrogen leaving the cell ($V_{H_2\,out}$) through the valve. The data from the measuring instruments were collected by a 16-channel computerized data acquisition system.

2. Thermal runaway phenomena (TRA)

2.1. Changes in I, T, φ^+, φ^- and ($V_{H_2\,out}$) with time of polarization at U = const

The TRA phenomena were investigated during a series of polarization runs of charged lead–acid cells from 2.65 to 2.40 V in 50 mV increments [19]. Fig. 3 shows the changes in all six measured parameters on cell polarization at 2.45 and 2.40 V.

Twelve minutes after the start of the polarization run at 2.45 V, the cell temperature began to rise slowly and after 18 min the current began to increase rapidly. After 45 min, the current reached the upper limit of the test equipment (9.5 A) and the polarization was interrupted. The cell temperature had reached

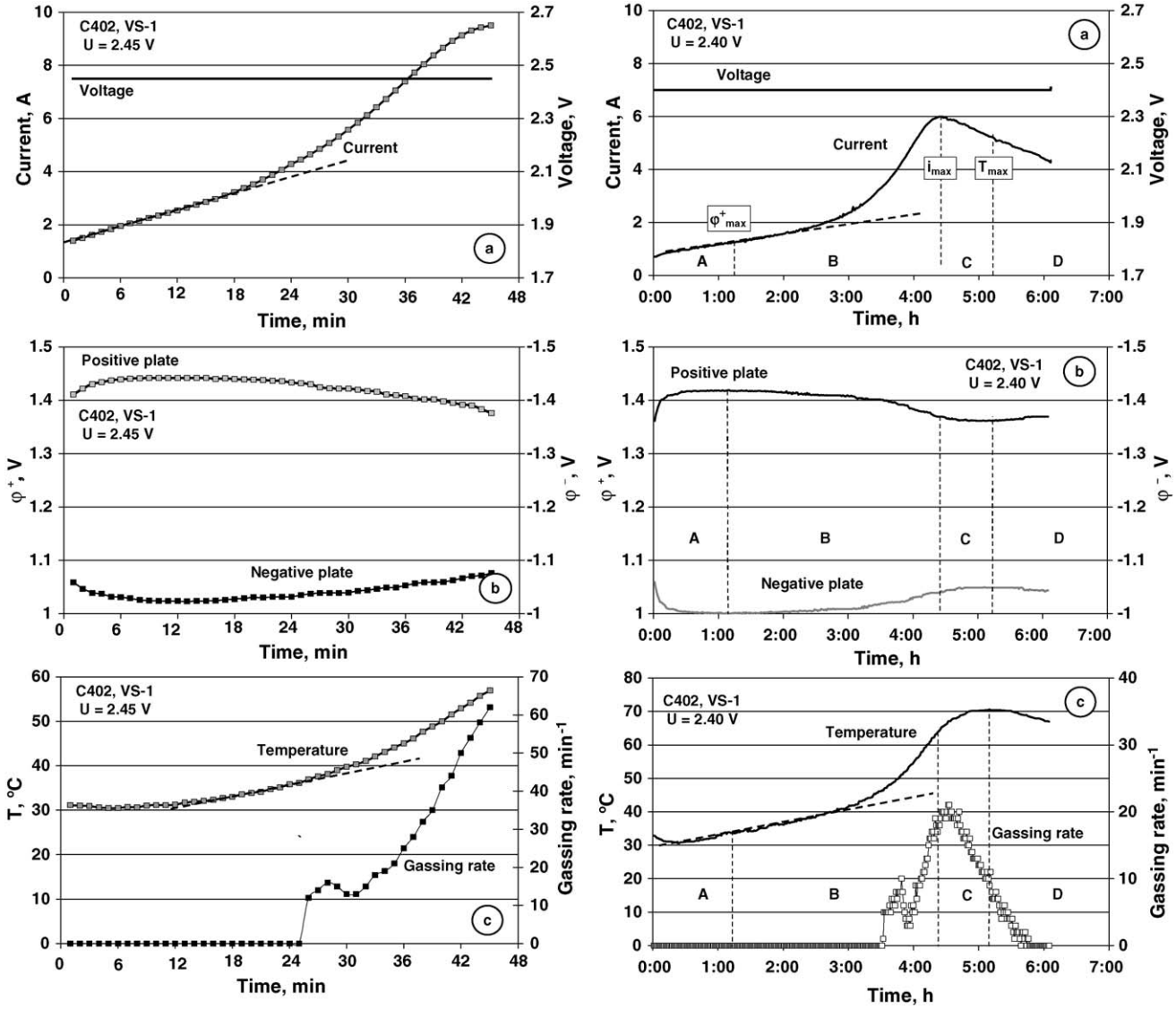

Fig. 3. Changes in potential of the positive (φ^+) and negative (φ^-) plates, current (I), temperature (T) and rate of gas leaving the cell on cell polatrization at 2.45 and 2.40 V [19].

57 °C. Twenty-five minutes after the beginning of polarization, gas began to be released from the cell at $I = 4.4$ A and $T = 35$ °C. The efficiency of the OxCy declined with increase in I and T.

2.2. TRA stages

At 2.40 V, after 1 h of polarization the potential of the positive plates passed through a maximum, while that of the negative plates passed through a minimum. After 4.5 h, both the current and the gassing rate passed through maxima and finally after 5.5 h of polarization, the temperature reached a maximum, too. The above maxima outline four stages in the development of the TRA phenomena. Let us designate the period from the beginning of polarization to the maximum potential of the positive plates as stage A, the period between the positive plate potential maximum and the current maximum as stage B, that between I_{max} and T_{max} as stage C, and the final stage after T_{max} as stage D. The latter stage ends with the beginning of the stationary stage in the OxCy operation.

2.3. SAIRE phenomena

During the A-stage, at the beginning of polarization, H_2 and O_2 are evolved on both plates. Oxygen is reduced on the negative plate. This process leads to a decrease in negative plate potential. To keep the cell voltage constant, the potential of the positive plate increases, which leads to an increase of the current of O_2 evolution.

Stage B starts after 2.5 h of polarization with a rapid spontaneous current increase followed by temperature rise. When O_2 is reduced on the negative plates, some heat is released and the temperature in the cell rises. At higher temperatures, the overpotential of O_2 evolution decreases, the current increases, a greater O_2 flow is generated and the rate of its reduction at the negative plates increases. More heat is released and hence the cell temperature rises. A loop involving the rates of the reactions of O_2 evolution and reduction at the two electrodes is formed (Fig. 4). The processes that occur at the two electrodes are in a positive interrelation, i.e. they accelerate each other [13].

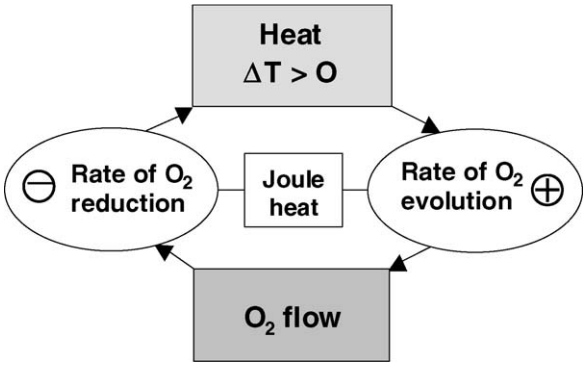

Fig. 4. Scheme of the processes at the two electrodes that are in positive interrelation (SAIRE). These processes accelerate each other forming a loop [13].

The above phenomena represent a Self-Accelerating Interrelation between the Reactions of O_2 formation at the positive and O_2 reduction at the negative Electrodes (SAIRE). The SAIRE phenomena lead to thermal runaway.

2.4. When does the SAIRE loop stop to operate?

During operation of the OxCy, the concentration of H_2SO_4 at the two interfaces changes. Water is consumed in the pores of lead dioxide active mass and hence the concentration of H_2SO_4 at the AGM/PAM interface increases. At the same time the reactions in the negative active mass result in the formation of water and consequently the concentration of H_2SO_4 at the AGM/NAM interface decreases. These processes lead to changes in the composition and structure of the electrode interfaces, which, in turn, may slow down the rates of the reactions or even cause the type of the reactions to change.

2.5. C and D stages of TRA

The elevated cell temperature and increased H_2SO_4 concentration at the positive plates lead to passivation of PAM and reduce the rate of the O_2 evolution reaction. The current passes through a maximum. Stage C starts.

Due to the elevated cell temperature a more intense heat exchange with the surrounding proceeds. After a certain period of time, the amount of heat leaving the cell and dissipating in the surrounding atmosphere becomes equal to the heat generated in the cell. The temperature reaches its maximum and starts to decrease. The D-stage starts. A negative interrelation is established between the processes at the two electrodes in the cell, until both the current and temperature reach stationary values.

3. Processes of O_2 evolution and their dependence on the structure of the PbO_2 electrode

3.1. Structure and phase composition of PbO_2 particles

As has been established earlier, lead dioxide particles and agglomerates comprise crystal zones of βPbO_2 and αPbO_2, and hydrated zones of $PbO(OH)_2$ formed by the reaction between PbO_2 and H_2O at the surface of particles and agglomerates [20]. The discharge processes (reduction of PbO_2) and the processes of oxygen evolution proceed in active centers in the hydrated zones. The active centers can be single structures in the particles or single particles in the agglomerates. The hydrated zones exchange water molecules and ions with the solution and the crystal zones and are open systems [21]. The phase composition of the particles depends on their size and shape, on cell temperature, H_2SO_4 concentration and type and concentration of ions contained in the solutions.

3.2. Mechanism of the reactions of O_2 evolution

According to the mechanism described in [14], oxygen evolution proceeds through the following elementary reactions in

the hydrated (gel) zones of PbO_2 particles and agglomerates:

$$PbO^{*}\cdot(OH)_2 + H_2O \rightarrow PbO^{*}\cdot(OH)_2\cdots(OH)^0 + H^+ + e^- \quad (E_F) \qquad (1)$$

$PbO^{*}\cdot(OH)_2$ is a hydrated active center. The obtained OH^0 radicals remain connected with the active centers. The latter become gradually saturated with OH^0 radicals and the electrode gets passivated. A very small anodic current flows due only to partial desorption of OH^0 radicals. Reaction (1) proceeds at potentials higher than $E_F = 1.1$ V versus Hg/Hg_2SO_4 electrode. When the potential exceeds a certain value (E_S higher than E_F), the second electrochemical reaction starts:

$$PbO^{*}\cdot(OH)_2\cdots(OH)^0 \rightarrow PbO^{*}\cdot(OH)_2 + O + H^+ + e^- \quad (E_S) \qquad (2)$$

The oxygen atoms evolved leave the active centers and reaction (1) proceeds again in the free active centers. The oxygen atoms accumulate in the hydrated zones and recombine according to the following reaction:

$$2O \rightarrow O_2 \qquad (3)$$

O_2 molecules leave the lead dioxide particles and agglomerates.

Beside through reaction (2) above, oxygen atoms can also result from the recombination of OH radicals, formed in the active centers by reaction (1), whereby the following chemical reaction proceeds:

$$2OH \rightarrow O + H_2O \qquad (4)$$

Oxygen atoms recombine through reaction (3) into O_2 molecules, which then form a gas phase.

3.3. Influence of T on the Tafel dependence of O_2 evolution

Voltammograms at 1 mV s^{-1} sweep rate at different temperatures are presented in Tafel co-ordinates in Fig. 5 [15].

With increase of temperature the curves shift to higher currents. Thus, on polarization at 1.28 V (versus Hg/Hg_2SO_4 electrode), when the temperature rises from 14 to 70 °C, the current increases by more than two orders of magnitude. The current

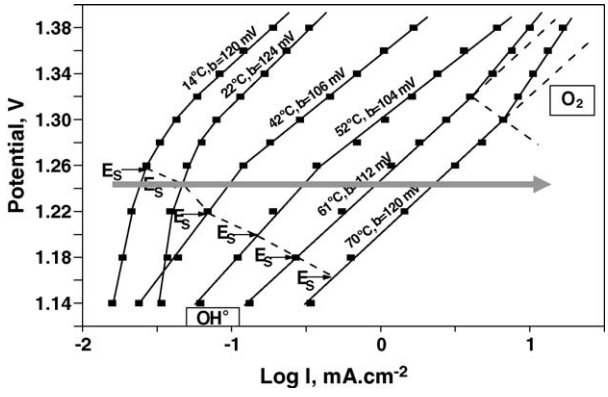

Fig. 5. Tafel plots at different temperatures of the oxygen evolution reaction [15].

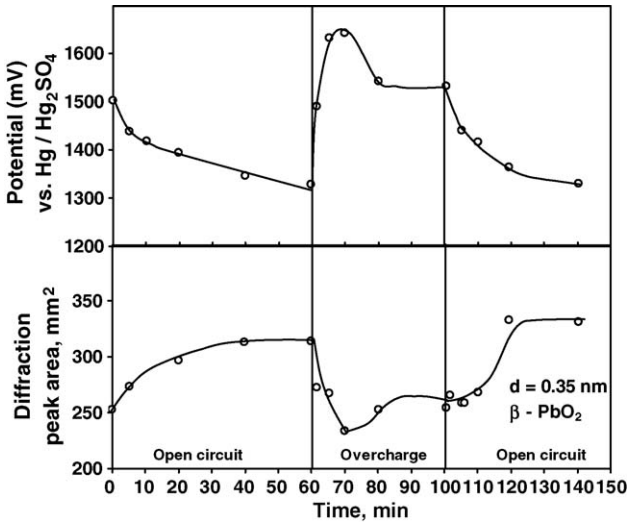

Fig. 6. Changes in positive plate potential and intensity of the characteristic diffraction line for βPbO_2 ($d = 3.50$ Å) on overcharge (oxygen reaction) and on open circuit [20].

increase is due to the lower overvoltage of O_2 evolution at elevated temperatures. These experiments were performed with single electrodes soaked in H_2SO_4 solution.

3.4. Influence of the rate of O_2 evolution on the crystallinity of PbO_2 particles

It has been established that the oxygen evolved at the PbO_2 plates of a lead–acid cell influences greatly the proportion between crystal and hydrated (gel) zones in PAM [20]. This influence is illustrated, in terms of changes in the amount of the βPbO_2 phase and in plate potential, in Fig. 6.

When the oxygen reaction proceeds through the above described mechanism, it yields OH radicals, O atoms and O_2 molecules. These diffuse into the PbO_2 particles and agglomerates thus creating a high concentration of structural defects. Part of the crystal structure of the βPbO_2 phase becomes amorphous. These transformations are demonstrated in the smaller area of the X-ray diffraction peaks in the X-ray patterns for βPbO_2. The potential of the PbO_2 plates increases substantially, which is an indication of impeded stages of the oxygen reaction. When the electric circuit is open, the reactions of oxygen evolution stop and the oxygen particles (O_2, O and OH) diffuse back from the solid phase to the gel zones and the solution. The crystal structures in the βPbO_2 phase are restored (the X-ray diffraction peaks for βPbO_2 become larger). The potential of the PbO_2 plates declines (Fig. 6).

3.5. Influence of T on the gel/crystal ratio and the shape of PbO_2 particles

Fig. 7 presents a picture of PbO_2 particles and agglomerates after operation of the PbO_2 plate at temperature higher than 60 °C (Fig. 7a) and a picture of PbO_2 particles and agglomerates after formation of the positive plate, when it delivers its rated capacity (Fig. 7b).

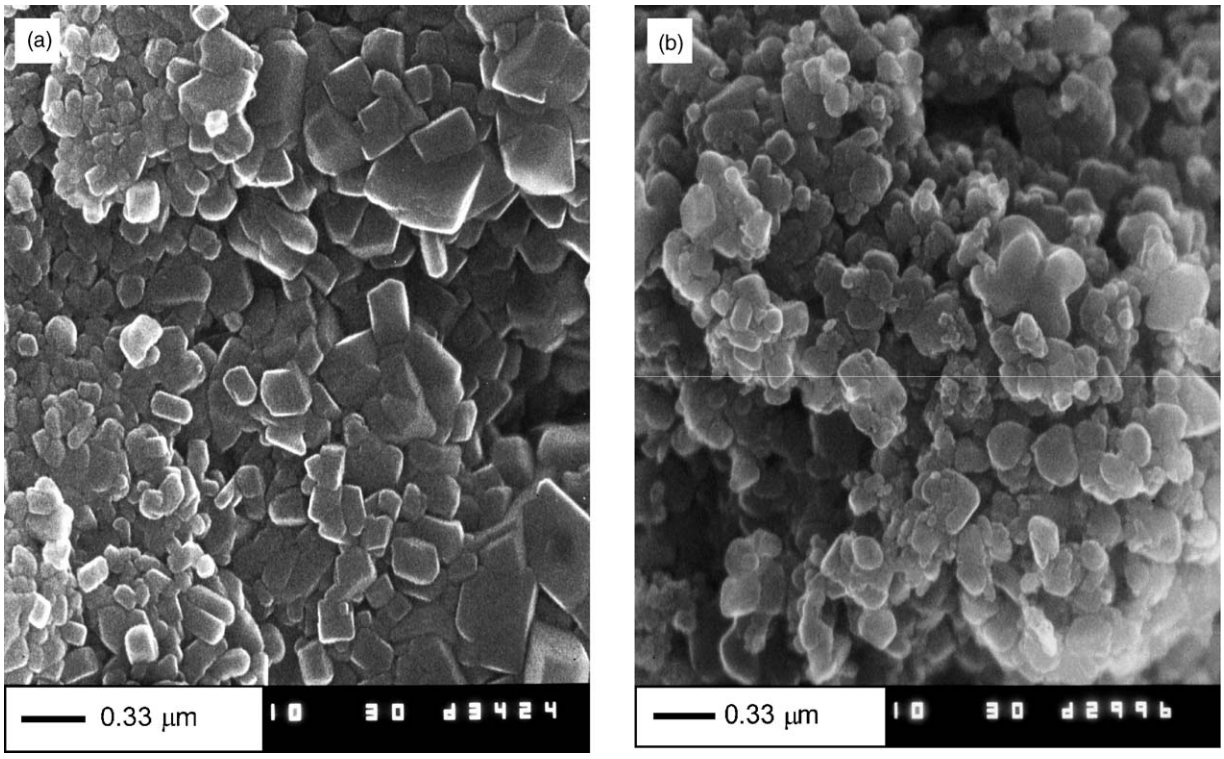

Fig. 7. SEM pictures of PbO_2 particles and agglomerates in PAM: (a) after thermal treatment at $t > 60\,^{\circ}C$ when the crystal zones determine the shape of the particles (electrochemically passive PbO_2) and (b) after plate formation when the hydrated (gel) zones give the shape of the particles (electrochemically active PbO_2).

When the volume of the hydrated zones has decreased substantially, the shape of the crystal zones determines the shape of the PbO_2 particles. When the hydrated zones predominate in the PbO_2 structure, the edges and apexes of the particles are rounded and the particles are drop-like in shape (Fig. 7b). In this case, the particles' shape is determined by the hydrated (gel) zones in them. Electrochemical reactions proceed in the gel zones. Hence, the gel/crystal ratio will influence strongly the electroactivity of the PbO_2 electrode [22,23]. The decreased volume of the hydrated zones (Fig. 7a) leads to a decrease in the number of active centers where the oxygen reactions proceed. Fig. 3 shows that the rate of the oxygen reaction reaches a maximum and begins to decline thereafter, despite the continuous temperature rise. From a kinetic point of view the rate of the reactions of oxygen evolution should increase with increase of temperature. However, the structural changes that have occurred in the PbO_2 particles with decrease of the volume of the hydrated zones (number of active centers) slow down the rate of the oxygen reactions (1)–(4). The electrode gets partly passivated.

3.6. Influence of $C_{H_2SO_4}$ on PbO_2 electrochemical activity

Fig. 8 shows the dependence of the electrochemical activity of PbO_2 (determined from the quantity of electricity flowing through the PbO_2 electrode on its reduction to $PbSO_4$) on the concentration of H_2SO_4 [24,25]. Three H_2SO_4 concentration regions can be distinguished:

(a) *Passive high concentration region*. This region includes concentrations higher than 5 M H_2SO_4 (1.28 s.g.). The anodic layer formed within this region has low electrochemical activity that decreases on further increase of the H_2SO_4 concentration. The crystal shapes of PbO_2 particles are very well pronounced.

(b) *Active medium concentration region*. This region covers concentrations between 5.0 and 0.5 M H_2SO_4 and yields electrochemically active βPbO_2 structures. It is within

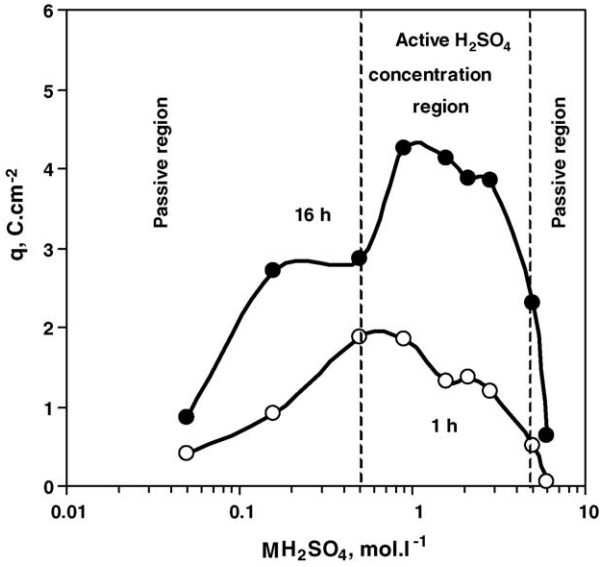

Fig. 8. Quantity of active PbO_2 (q, C cm^{-2}) that is reduced, depending on the concentration of H_2SO_4. The electrode was cycled for 1 and 16 h [16].

this concentration region that the positive electrode of the lead–acid battery operates.

(c) *Passive low concentration region*. It includes concentrations below 0.5 M H_2SO_4.

3.7. Influence of $C_{H_2SO_4}$ on the composition of the hydrated zones

Though the thus determined electrochemical activity refers to the lead current generating and accumulating system, it could be assumed that it would also influence strongly the oxygen reaction as the latter proceeds in the same hydrated zones. Hydrated zones and the solution exchange ions and the following reactions may proceed [21]:

$$PbO(OH)_2 + H_2SO_4 \leftrightarrow PbOSO_4 + 2H_2O$$

$$PbO(OH)_2 + 2H_2SO_4 \leftrightarrow PbO(HSO_4)_2 + 2H_2O$$

It is well known that PAM adsorbs readily SO_4^{2-} and HSO_4^- ions [26,27]. Due to these processes the concentration of the active centers in the hydrated zones decreases, which slows down the rate of O_2 evolution. Hence, the increased H_2SO_4 concentration at the interface AGM separator/PbO_2 plate and in the PAM pores will lead to the formation of a passive PbO_2 which will yield a maximum in the current transient followed by subsequent current decline, as evidenced in Fig. 3.

4. Processes at the negative plate during operation of the oxygen cycle

4.1. Two types of O_2 reduction reactions

Oxygen reduction proceeds at the negative plates through electrochemical and chemical reactions. The nature of these reactions can be judged by the temperature dependence on the current passing through the cell at various voltages. Fig. 9 presents the temperature/current function for six different voltages between 2.65 and 2.40 V. Polarization of the cell started at 2.65 V and the voltage was reduced by 50 mV after each polarization run [19]. The current was limited to 9.5 A during each run.

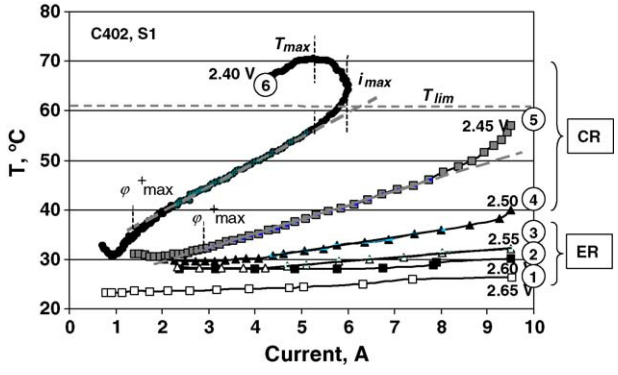

Fig. 9. Dependence of temperature on the current flowing through the cell at six different voltages applied to the cell [19].

Judging by the temperature increase as a function of current, we can distinguish two regions:

(a) ER region (runs 1–3)—the temperature increase is small for increase of current up to 9.5 A = 2.1C_{10} A;

(b) CR region (runs 4–6)—the temperature increase is substantial for the same current increase. At 2.40 V, the maxima T_{max} and I_{max} appear.

This behaviour of the *T*/*I* curves indicates a change in the nature of the reactions that proceed during the reduction of O_2.

4.2. ER region: O_2 reduction through electrochemical reactions

Within the ER region, the OxCy operates at high rate, but no heat is generated and the temperature increases but very slightly. This is possible only if reversible electrochemical reactions proceed. In this case, the energetic transformations involved in the OxCy are as follows. At the positive plates, the electrical energy is converted into chemical energy through the electrochemical reaction of oxygen evolution. At the negative plates, the oxygen is reduced to water through electrochemical reactions and the chemical energy is converted into electrical energy. The OxCy involves only electrochemical reactions of O_2 formation and reduction. To confirm this hypothesis we determined the amounts of heat generated by the chemical reactions and that due to the Joule effect.

4.3. Thermal effects on electrochemical oxygen reduction within the ER region

With the help of calorimetric calculations we determined the total heat (Q) generated in the cell on polarization at 2.65 V as well as the Joule heat (Q_J) [19]. The equations presented by Gu and Wang in [28] were used for these calculations. The difference between these two heats gives the heat released only by the reactions of the OxCy ($Q_r = Q - Q_J$).

Fig. 10 shows the changes in all three types of heats with time of polarization as calculated in [19]. The reaction heat is negligible. The predominant heat is that generated by the Joule effect. Hence, the reduction of O_2 at 2.65 V (high voltage polarization at *I*) proceeds through electrochemical reactions and the cell temperature does not increase much. This region was called "electrochemical region" (ER).

4.4. CR region: O_2 reduction through chemical reactions

Fig. 9 evidences that, though the cell polarization is conducted at lower voltages than those in the ER region, the cell temperature rises rapidly. At 2.40 V, all four stages of the TRA phenomenon exhibit clearly.

Fig. 11 shows the changes in the generated heats during polarization of the cell at 2.40 V calculated using the equations proposed by Gu and Wang [28]. The major part of the heat is generated by the exothermic reactions and only a small part is a result of the Joule effect. Exothermic chemical reactions are

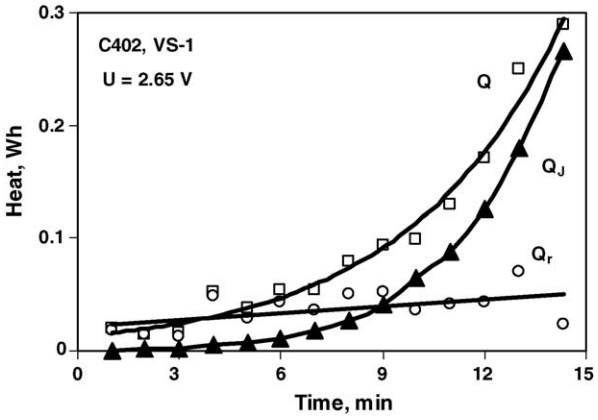

Fig. 10. Changes in the total amount of generated heat (Q) and the Joule heat (Q_J) on cell polarization at 2.65 V. Q is calculated from calorimetric data. Q_r is the heat generated by the reactions of O_2 reduction and calculated as the difference $Q_r = Q - Q_J$ [19].

involved in the reduction of oxygen. Hence, this region was called "chemical region" (CR).

4.5. Dependence of T and I on Q at different U

Fig. 12 presents the current and temperature as a function of the quantity of electricity on cell polarization between 2.65 and 2.40 V.

Both I and T increase linearly during the A stage (Fig. 12a and c). The slope dI/dQ depends on the cell voltage: the higher the voltage the steeper the slope. When a certain quantity of electricity flows through the cell, i.e. a definite electrolyte concentration is reached at the interface lead surface/electrolyte layer and a definite structure of the Pb surface is obtained, a spontaneous increase in I and T starts at 4.2 Ah for the current and at 4.6 Ah for the temperature, respectively ($U = 2.40$ V, Fig. 12b and d). These values are higher than the values at the end of polarization at higher voltages presented in Fig. 12a and c. In the latter case, the changes in H_2SO_4 concentration in the NAM pores are not sufficient to induce changes in the structure of NAM that would initiate exothermic chemical reactions.

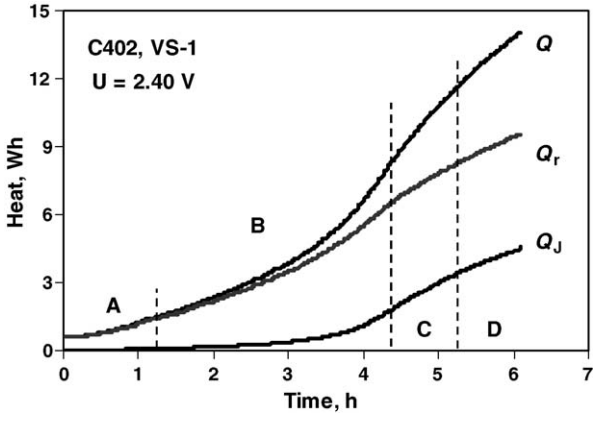

Fig. 11. Changes in the total amount of generated heat (Q), the Joule heat (Q_J) and the heat generated by the reactions (Q_r) on cell polarization at 2.40 V [19].

Fig. 12c evidences that, within the A stage, the slope dT/dQ depends but very slightly or is almost independent of cell voltage. The heat generated in the cell is a result mainly of the Joule effect.

4.6. When do I_{max} and T_{max} appear?

To find an answer to this question we conducted several series of polarizations between 2.65 and 2.40 V [19]. Fig. 13a presents the obtained T versus I functions at different cell voltages at which TRA occurs. Fig. 13b shows the dependences of I_{max} and T_{max} on cell voltage.

The data in this figure evidence that with increase in polarization voltage T_{max} increases linearly, whereas I_{max} passes through a maximum at 2.50 V and decreases thereafter (Fig. 13b). At 2.65 V during the third series of polarization tests, a second maximum occurs in the current transient (Fig. 13a). This maximum is related to re-activation of the cell. This behaviour of the T/I curve is an indication of changes in the type of reactions that proceed at the negative plates and of passivation phenomena that occur at the positive plates.

4.7. Phase composition of NAM after OxCy operation

Fig. 14 presents XRD patterns for lead active mass (NAM) samples taken from the upper and lower parts of the negative plates on completion of the test [19].

It can be seen that considerable amounts of $PbSO_4$ have formed in the upper part of the plates, whereas in the lower part, beside $PbSO_4$, 3BS and PbO are detected as well. Since these latter compounds form at different pH, it can be presumed that the electrolyte filling the different pores in NAM reaches different pH values during operation of the OxCy.

The above identified composition of NAM indicates that the process of O_2 reduction at the negative plates involves also Pb, whereby the electrochemical reduction of $PbSO_4$, 3BS and PbO to Pb is slowed down in some regions of NAM. These compounds are actually detected by the XRD analysis. The obtained amounts of $PbSO_4$, PbO and 3BS as well as the amount of the H_2 released from the cell are equivalent to the amount of the water loss during operation of the OxCy.

5. Reactions of O_2 reduction at the negative plates

5.1. Formation of H_2O_2 and $Pb(OH)_2$ as intermediate products

The energy binding the oxygen atoms in molecules is high. At room temperature, these bonds can be broken through the formation of an intermediate product [29]. This occurs through an electrochemical reaction of formation of H_2O_2 [16] or through a chemical reaction of oxidation of lead and formation of PbO or $Pb(OH)_2$. Fig. 15 proposes a scheme of the electrochemical and chemical reactions taking into account the products detected by the XRD analysis (Fig. 14) and the electrochemical behaviour of the cell presented in Fig. 3 as well as the results of our earlier paper [16].

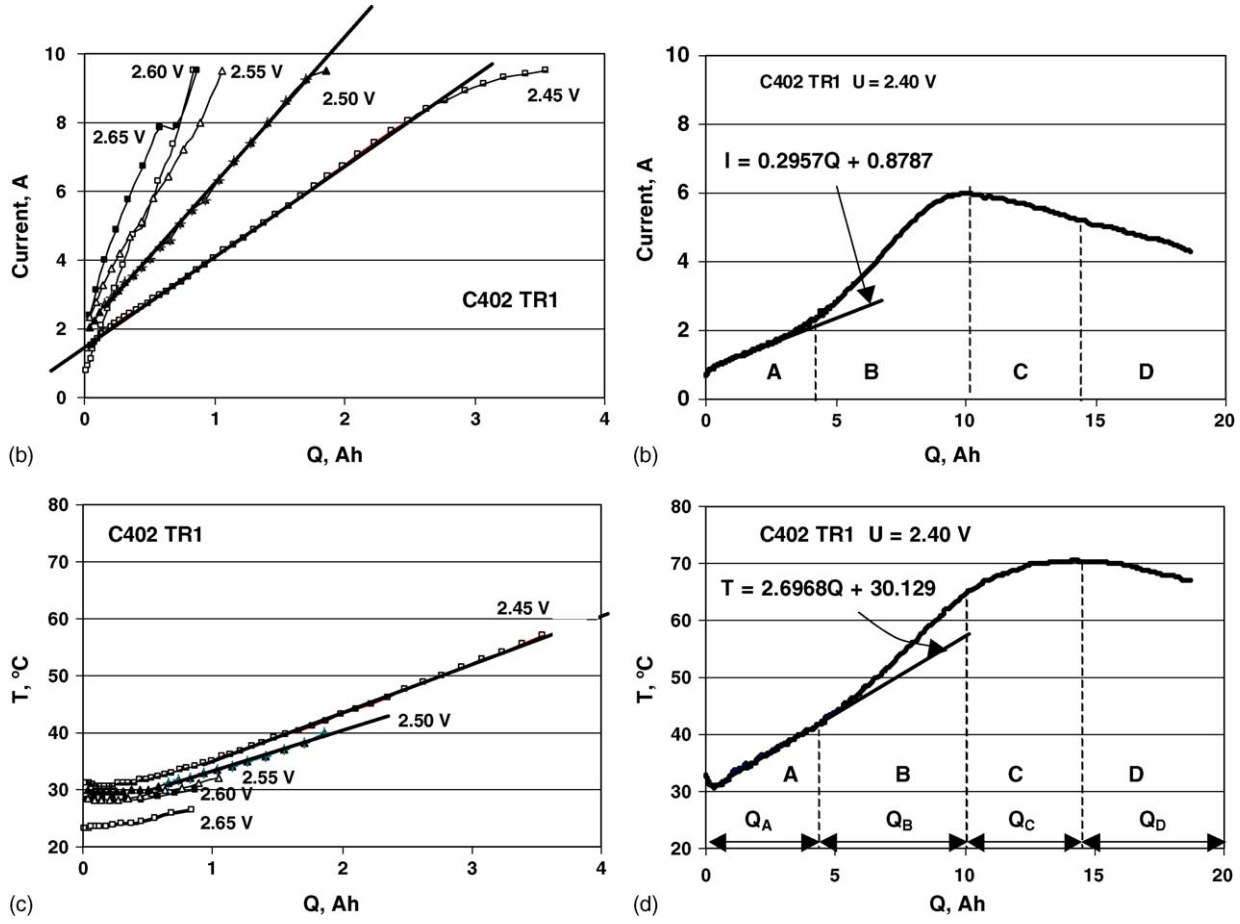

Fig. 12. Dependence of current and temperature on the quantity of electricity (Q) flowing through the cell at six different polarization voltages [19].

5.2. Thermodynamic evaluation of the reactions

The scheme in Fig. 15 illustrates the changes in enthalpy (heat effect of the reactions at 1 atm pressure and 25 °C) of the chemical reactions. The leading negative sign of the heat effect indicates that the reaction is exothermic. In the case of electrochemical reactions, the chemical energy is mainly converted into electrical one and only a small amount is released in the form of heat (Figs. 9 and 10). That is why the changes in enthalpy of this type of reactions are not given in the scheme. Most of the initial thermodynamic data have been taken from [30].

Table 1 presents the Gibbs free energies (ΔG°) for the respective reactions. The negative sign preceding ΔG° indicates that

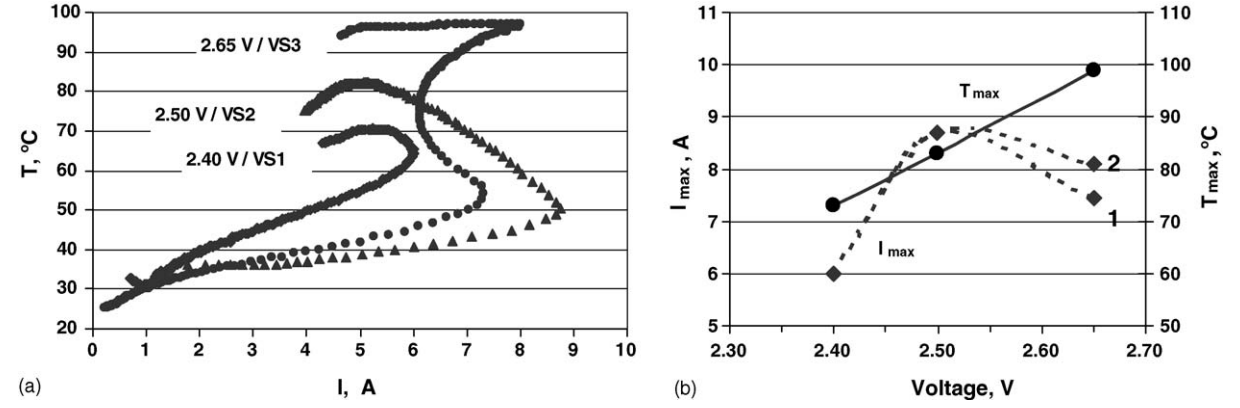

Fig. 13. (a) Dependence of cell temperature on current during three different polarization series with TRA [19] and (b) I_{max} and T_{max} as a function of the voltage applied to the cell.

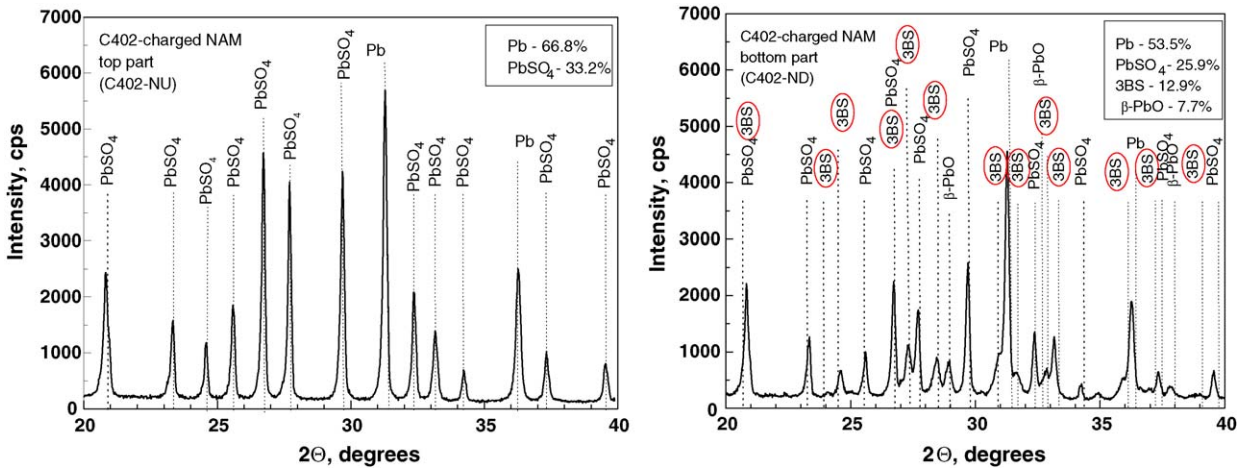

Fig. 14. X-ray diffractograms of the negative active mass in the upper and lower parts of the plates after prolonged operation of the OxCy [19].

these reactions proceed spontaneously, provided there are no kinetic hindrances.

5.3. Reactions of H_2O_2 formation and reduction

The mechanism of the reactions yielding H_2O_2 as an intermediate product was proposed in [16]. First, the electrochemical reaction (5) proceeds, which results in the formation of H_2O_2. The latter may take part in four types of reactions. This is a second electrochemical reaction (6), which yields water. The above processes proceed in the ER region (Figs. 9 and 10). When the temperature and the potential of the negative plates rise, the overvoltage of hydrogen evolution is reduced and hence the evolution of hydrogen (reaction (8)) is accelerated. Hydrogen is a strong reducer and H_2O_2 is a strong oxidizer. Part of the hydrogen reacts with H_2O_2 according to reaction (7) forming water and heat is released (383.2 kJ mol^{-1}). The remaining part of hydrogen forms H_2 molecules (reaction (9)) and leaves the cell in the form of gas, provided the rate of reaction (7) is slower.

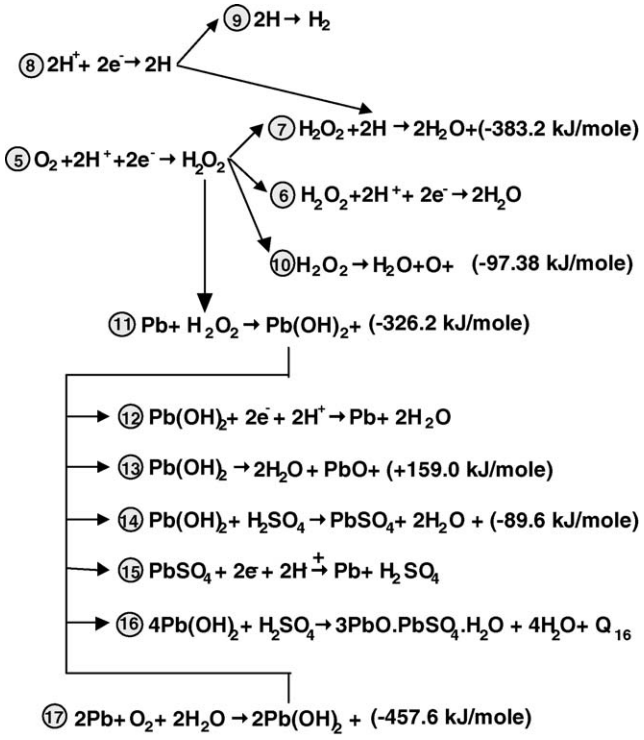

Fig. 15. Scheme of the chemical and electrochemical reactions involved in the reduction of oxygen at the negative plates.

5.4. Catalytic H_2O_2 decomposition

A reaction of H_2O_2 decomposition (reaction (10)) is also possible (Table 1), which will result in the formation of water and oxygen. This reaction is also exothermic and is catalyzed by some noble metals. There is no data available in the literature about the catalytic effect of lead. If the above reaction proceeds, the generated oxygen may oxidize the lead to PbO.

5.5. Oxidation of Pb by H_2O_2 and formation of $Pb(OH)_2$

H_2O_2 may react with Pb through reaction (11) yielding $Pb(OH)_2$ and heat is released (326.2 kJ mol^{-1}). Thus, the H_2O_2 formed by reaction (5), is involved in reactions (6), (7), (10) and (11) under certain conditions in the NAM pores and heat is generated by reactions (7), (10) and (11), which leads to temperature rise (CR region, Figs. 9 and 11).

$Pb(OH)_2$ may take part in the electrochemical reaction (12), get dehydrated according to the endothermic reaction (13) yielding PbO (registered by XRD, Fig. 14), react with H_2SO_4 through reaction (14) forming $PbSO_4$. The latter is detected by the XRD

Table 1
Changes in Gibbs free energy during the reactions presented in Fig. 15

Reaction number (according to Fig. 14)	ΔG° (kJ mol^{-1})
7	−354.0
10	−116.8
11	−300.5
13	−242.4
14	−111.3
17	−371.5

analysis throughout the volume of the plate (Fig. 14). $PbSO_4$ may then be reduced to Pb (reaction (15)). When the H_2SO_4 concentration in some pores is lower, sulfation of $Pb(OH)_2$ yields $3PbO{\cdot}PbSO_4{\cdot}H_2O$, which is also detected in NAM though in small amounts (Fig. 14). Reactions (13), (14) and (16) are exothermic and the heat released contributes to the temperature rise.

5.6. Oxidation of Pb by O_2

The second mechanism of breaking the bonds between the O atoms in the O_2 molecule is through the chemical reaction of direct Pb oxidation (reaction (17)) resulting in the formation of $Pb(OH)_2$. This reaction, too, has a substantial heat effect ($457.6\,kJ\,mol^{-1}$). $Pb(OH)_2$ takes part in reactions (12)–(16).

Depending on the conditions created in the different pores in NAM, different reactions may proceed and at different rates. Most of the reactions result in the formation of water that dilutes the electrolyte in the pores of NAM and changes the nature of the reactions.

5.7. Hess law and mechanism of the OxCy reactions

Hess law reads: when chemical or electrochemical reactions proceed in one system the changes in its energy do not depend on the type of the reactions if the initial and final products of the reactions are the same and they proceed at constant temperature and pressure or volume. Figs. 3, 9 and 13 show that during OxCy operation the cell temperature increases significantly. Figs. 3 and 15 demonstrate that beside water H_2, $PbSO_4$, 3BS, and PbO are also formed on the negative plate, hence the end product of the oxygen reduction is not only water. This means that Hess law is not valid for the OxCy.

5.8. Sulfation of the negative plates during OxCy operation

When stationary VRLA batteries were first introduced in the battery practice, it was established that after several years of float service the batteries lost capacity because of sulfation of the negative plates. This was a result of the above chemical reactions involved in the OxCy. The sulfation can be "cured" by adding certain amounts of water to the cells, so as to restore the water loss, and by re-charging the battery to allow $PbSO_4$, PbO and 3BS to convert into Pb. The above "curing" procedure can be controlled by measuring the electro-conductivity of the cell.

So, during operation of the OxCy in VRLAB, the reduction of O_2 to water proceeds with certain capacity loss of the negative plates. Part of the O_2, together with an equivalent amount of H_2 leaves the cell, which results in water loss. Another part is involved in the oxidation of the Pb plate leading to its discharge (sulfation).

6. Influence of AGM separator on the occurrence of TRA

The separator is the medium through which the flows of O_2 and H^+ ions, involved in the OxCy and the SAIRE phenomena, are transported. Thus, the separator thickness and properties play a crucial role for the occurrence and the progress and magnitude of the TRA phenomenon.

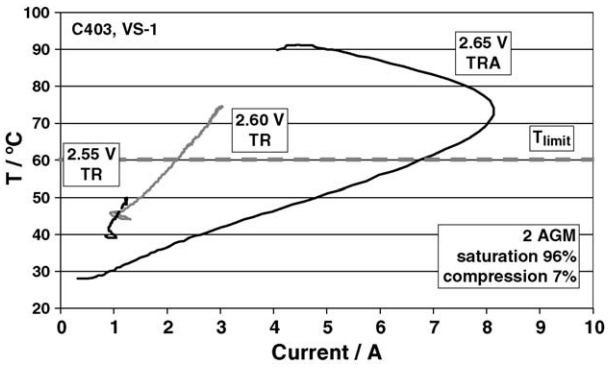

Fig. 16. Dependence of temperature on current for cell with two layers of AGM separator polarized at different voltages [19].

6.1. Influence of AGM separator thickness on TRA

Fig. 16 presents T versus I curves for VRLA cells assembled with two layers of AGM separator (2AGM) [19]. The higher cell voltages were chosen so as to allow the TRA to manifest fully.

The data in Fig. 9 evidence that the TRA appears at 2.40 V for cells assembled with one layer of AGM separator (1AGM) against 2.65 V for the 2AGM cells (Fig. 16). At lower cell voltages (2.60–2.50 V), the temperature increases to a steady state value $T_{st} < 70\,^{\circ}C$. Hence, the initiation of the SAIRE loop depends on the thickness of the separator: the thicker the separator the higher the voltages at which the TRA occurs. This is quite logical to expect since the development of the SAIRE phenomena depends on the oxygen flow, which is impeded by the higher resistance of the thicker separator. A practical conclusion can be drawn: the TRA phenomenon can be avoided through appropriate increase of the AGM separator thickness and by limiting the cell voltage to a definite level.

6.2. Influence of separator physico-chemical properties on TRA

In our laboratory we modified standard AGM separator with polymer emulsion [31]. The new product called MAGM has new physico-chemical properties. Experiments analogous to those performed with 1 AGM separator were conducted using cells assembled with one layer of MAGM separator (1MAGM). The obtained T versus I curves are presented in Fig. 17.

TRA occurs only at the highest polarization voltage 2.65 V. At lower voltages (2.60–2.45 V), only temperature rise is observed. The MAGM separator suppresses the TRA phenomena and demonstrates that it is possible to control the TRA phenomena through an appropriate choice of separator type and thickness.

6.3. Critical I_{max} during TRA

The upper temperature limit for normal operation of VRLA batteries is 60 °C. At higher temperatures, the expander disin-

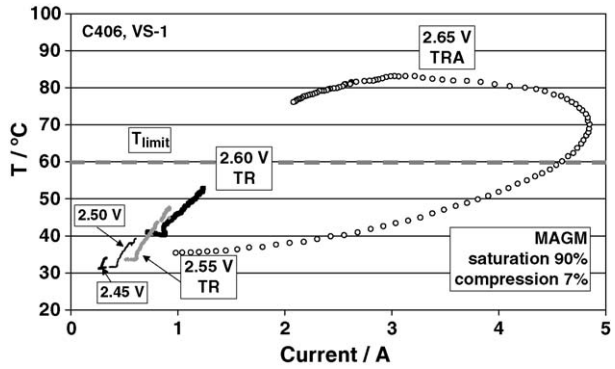

Fig. 17. Dependence of temperature on current for cell with one layer of MAGM separator polarized at different voltages [19].

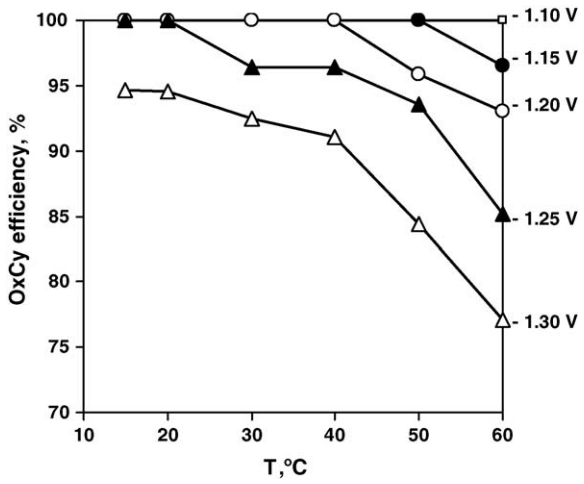

Fig. 18. Dependence of OxCy efficiency on temperature during reduction of O_2 at different negative plate potentials [18].

tegrates, water starts to evaporate intensively, etc. The data in Figs. 9, 16 and 17 indicate that in order to prevent the cell temperature from rising beyond the above limit when TRA occurs, I_{max} should be kept down below $1C_{10}$ A. Under such conditions, T_{max} does not exceed 60 °C and no battery damages are to be expected. This can be achieved by reducing the cell voltage, limiting the current or increasing the internal electrical resistance of the battery.

7. Dependence of the OxCy efficiency on temperature and negative plate potential

7.1. Efficiency of the OxCy (η_{OxCy})

It can be calculated by the following equation:

$$\eta_{OxCy} = (I_{OxCy} \times 100)/I$$

where I is the current flowing through the cell and I_{OxCy} is the current involved in the OxCy. The latter current is determined from the difference $I_{OxCy} = I - I_{H_2\,out}$, where $I_{H_2\,out}$ is the calculated rate of the H_2 flow leaving the cell. It was measured experimentally with the help of a flowmeter [18].

The dependence of OxCy efficiency on T at $\varphi^- = \text{const}$ is presented in Fig. 18.

These results indicate that there is a certain critical temperature above which η_{OxCy} is a function of temperature and it declines with temperature increase. The value of this critical temperature depends on the potential of the negative plates: the higher the potential the lower the temperature above which η_{OxCy} declines. Thus, at $\varphi^- = 1.20$ V, the oxygen cycle is 100% efficient up to 40 °C. Above this temperature, η_{OxCy} declines rapidly. Hence, the negative plate potential is an important parameter, which strongly affects the thermal phenomena during OxCy operation. To avoid the appearance of TRA φ^- should be lower than −1.20 V (versus $Ag/AgSO_4$ electrode). When $\varphi^- > -1.25$ V, the oxygen reduction reactions at the negative plate are accompanied by a number of side reactions, most of them being exothermic, which impairs the OxCy efficiency, causes the cell temperature to rise and may cause TRA.

8. Conclusion

By monitoring six parameters (U, I, T, φ^-, φ^+, and V_{gass}) of VRLA cells polarized at high voltages (between 2.40 and 2.65 V), the processes that cause thermal phenomena and may generate TRA with undesirable effects to the cell performance were revealed. On grounds of the experimental results obtained, a model of the processes causing TRA is proposed. A positive interrelation is established between the rates of the reactions at the two electrodes, which leads to self-accelerated current and temperature increase. Due to passivation of the positive plate the current reaches a maximum. The temperature rise is a result of changes in the mechanism of oxygen reduction reactions at the negative plates—electrochemical reactions are replaced by exothermic chemical reactions. This causes the efficiency of the OxCy to decline and leads to water loss and cell temperature rise. The latter may reach values above the critical temperature for normal lead acid cell operation. By choosing AGM separators of appropriate thickness and type as well as by limiting the cell voltage (to a level that does not allow the negative plate potential to reach its critical value), it is possible to suppress the thermal phenomena so as to avoid cell temperature rise above the critical value beyond which there is a serious battery safety hazard. In this way, TRA will be prevented or, even if it does occur, it will be restrained within the temperature interval of normal battery operation.

References

[1] H. Giess, J. Power Sources 67 (1997) 49.
[2] P. Haering, H. Giess, J. Power Sources 95 (2001) 153.
[3] A. Pesaran, M. Keyser, Proceedings of the 16th Battery Conference: Advances and Applications, Long Beach, CA, USA, 2001.
[4] A. Pesaran, A. Vlahinos, S.D. Burch, Proceedings of the 14th Electric Vehicles Symposium, Orlando, FL, USA, 1997.
[5] A. Pesaran, D.J. Russel, J.W. Crawford, R. Rehn, E.A. Lewis, Proceedings of Annual Battery Conference, Long Beach, CA, USA, 1998.
[6] B. Culpin, J. Power Sources 133 (2004) 79.
[7] R. Wagner, J. Power Sources 53 (1995) 153.

[8] Z. Li, Y. Guo, L. Wu, M. Perrin, H. Doering, J. Garche, J. Electrochem. Soc. 149 (2002) A934.
[9] R.S. Robinson, J.M. Tarascon, J. Power Sources 48 (1994) 277.
[10] S.D. Gerner, G.H. Brilmyer, D.H. Bornemann, Proceedings of INTELEC'90 Conference, 1990, p. 161.
[11] A.I. Harrison, Proceedings of INTELEC'92 Conference, 1992, p. 28.
[12] S.S. Misra, T.N. Noveske, A.W. Williamson, Proceedings of INTELEC'92 Conference, 1992, p. 186.
[13] D. Pavlov, J. Power Sources 64 (1997) 131.
[14] D. Pavlov, B. Monahov, J. Electrochem. Soc. 143 (1996) 3616.
[15] D. Pavlov, B. Monahov, J. Electrochem. Soc. 145 (1998) 70.
[16] D. Pavlov, A. Kirchev, B. Monahov, J. Power Sources 144 (2005) 521.
[17] A. Kirchev, D. Pavlov, B. Monahov, J. Power Sources 113 (2003) 245.
[18] A. Kirchev, D. Pavlov, J. Power Sources, in press, doi:10.1016/j.jpowsour.2005.07.008.
[19] D. Pavlov, B. Monahov, A. Kirchev, D. Valkovska, J. Power Sources 158 (2006) 689–704.
[20] D. Pavlov, I. Balkanov, T. Halachev, P. Rachev, J. Electrochem. Soc. 136 (1989) 3189.
[21] D. Pavlov, I. Balkanov, J. Electrochem. Soc. 139 (1992) 1830.
[22] D. Pavlov, J. Electrochem. Soc. 139 (1992) 3075.
[23] P. Faber, Electrochim. Acta 26 (1981) 1435.
[24] B. Monahov, D. Pavlov, A. Kirchev, S. Vasilev, J. Power Sources 113 (2003) 281.
[25] D. Pavlov, A. Kirchev, M. Stoycheva, B. Monahov, J. Power Sources 137 (2004) 288.
[26] P. Ruetschi, J. Ockerman, R. Amlie, J. Electrochem. Soc. 107 (1960).
[27] B.N. Kabanov, E.S. Weisberg, L.I. Romanova, E.V. Krivolapova, Electrochim. Acta 26 (1981) 1435.
[28] W.B. Gu, C.W. Wang, J. Electrochem. Soc. 9 (1964) 1197.
[29] M.C. Davies, M. Clark, E. Jeger, F. Hovorka, J. Electrochem. Soc. 106 (1959) 56.
[30] H. Bode, Lead–Acid Batteries, John Wiley & Sons, 1977, Appendixes 4–6, pp. 366–371.
[31] D. Pavlov, V. Naidenov, S. Ruevski, V. Mircheva, M. Cherneva, J. Power Sources 113 (2003) 209.